Development of a National Ignition Facility Laser Configuration with X-Ray Backlighting for Direct-Drive of a Foam Ball Target

Alisha Upal

Pittsford Sutherland High School

Pittsford, NY

Advisor: Dr. R. S. Craxton

Laboratory for Laser Energetics

University of Rochester

Rochester, New York

November 2022

Abstract

A laser configuration was developed for a National Ignition Facility (NIF) experiment that will compress an 1100 μm foam ball target. Foam ball targets are technology that may have applications in future fusion energy plants. Two quads, consisting of 4 beams each, are used for x-ray backlighting in order to obtain more extensive diagnostics on the foam ball, one quad in the upper hemisphere and one in the lower hemisphere. The backlighting quads are expected to produce an image of the target's shell which will be formed during the experiment. During compression, uniformity of a converging shock wave is necessary for a successful outcome. It was therefore essential to compensate for the backlighting beams and repoint the NIF beams in the θ (longitudinal) and φ (latitudinal) directions. The 2D hydrodynamics simulation code SAGE was used, maximizing the uniformity of the target's implosion. These simulations found velocity nonuniformity values for the shock wave as low as 1.40% RMS. The new laser pointing design is expected to be applicable to a variety of experiments that require beams to be used for backlighting.

1. Introduction

Nuclear fusion is a process that releases large amounts of energy through the combining of multiple atoms. Fusion provides a long-term, sustainable, safe energy source and is the primary objective of facilities like the National Ignition Facility (NIF). Inertial confinement fusion is one approach towards achieving nuclear fusion.[1] In inertial confinement fusion, laser beams or laser-produced x-rays irradiate a small target shell filled with fuel of two hydrogen isotopes, deuterium-tritium (DT), as illustrated in Figure 1(a). As the surface of the target reaches high temperatures, a plasma envelope is formed. This hot plasma wraps around the target. Next, in Figure 1(b) the hot shell is shown ablating outward and the internal fuel is consequently compressed from this force. The fuel reaches both extreme temperature and density, which leads to the hydrogen nuclei overcoming their repulsion forces and fusing as shown in Figure 1(c). A helium atom is formed and a neutron is released. The energy of the helium atom heats more of the compressed fuel, initiating a chain reaction and leading to "burn" where the kinetic energy of the neutron and helium atom produce a yield that is significantly larger than the input energy. This is labeled in Figure 1(d).

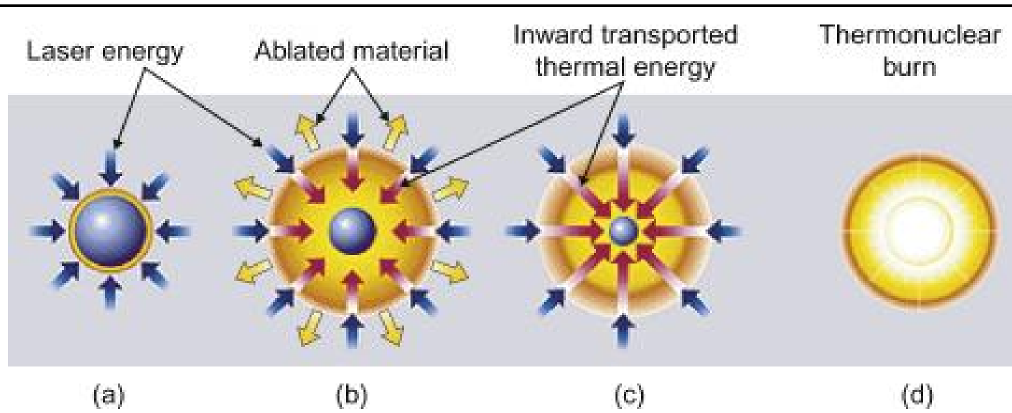

Figure 1: *Diagram of the steps in laser-driven nuclear fusion [From Ref. 1]*

The NIF and the OMEGA laser at the Laboratory of Laser Energetics (LLE) were constructed with a primary focus on two different methods for laser-driven nuclear fusion, which are indirect and direct drive respectively. For the direct drive method, shown in Figure 1, laser beams are aimed directly towards the target, also known as the capsule.[2] The laser beams irradiate the capsule at normal incidence. LLE employs the method of direct drive, which is considered more efficient than the indirect alternative. At LLE, the main laser system is called OMEGA which is an example of direct drive. OMEGA has 60 beams and provides up to 30 kJ of energy. In contrast, the NIF has 192 beams and gives up to 1.8 MJ of energy. LLE also has the OMEGA EP laser, which consists of 4 beams separate from OMEGA. It is capable of providing additional pulses to the OMEGA target chamber.

Indirect drive uses a hohlraum, typically made from gold due to its high atomic number, placed around the target.[3] This setup is shown in Figure 2. Laser beams must go through the holes at the ends of the hohlraum, and then upon impact with the walls of the hohlraum, the laser energy is converted to x-rays. It is the x-rays that then irradiate the capsule instead of the laser beams in direct drive. This method is less efficient because in the end the capsule absorbs roughly a fifth of the original energy from the laser beams. Most of the energy is absorbed by the hohlraum itself or is lost by escaping through the holes. However, the indirect drive method is prone to fewer perturbations and implosion nonuniformity issues. These issues arise from laser imperfections, thus direct drive is more sensitive to hydrodynamic instability.

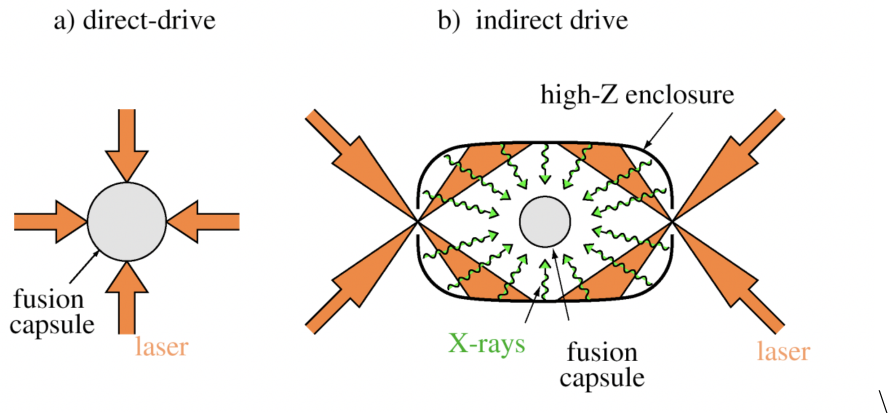

Figure 2: *A comparison between (a) direct drive and (b) indirect drive using a hohlraum, a high-Z enclosure that converts the laser energy to x-rays [From Ref. 4]*

The goal of these facilities and their projects is achieving nuclear fusion to support humanity's energy consumption. In a nuclear fusion reactor, targets would be expected to be fired at rates close to one target per second. Currently, conventional targets for direct drive are cryogenic plastic thin-shell spheres with DT ice layers inside. Producing one of these targets can take an entire day. The targets used in indirect drive have similar issues compared to the direct drive targets, regarding the inefficiency of their preparation time. The hohlraum used in the indirect drive method poses additional complications, which include requiring more preparation and depositing debris. The hohlraum material composes the majority of the mass of the target.

Alternative concepts such as the foam ball target are being explored to resolve these issues. Foam targets have an advantage of simplicity that would allow them to serve as better candidates for future fusion energy plants.[5] Instead of requiring the process to form DT ice layers, the foam ball targets only have to absorb liquid DT. Moreover, foam ball targets do not have a shell in their design. While conventional targets have pre-made plastic shells, for foam ball targets, the laser pulse forms the shell during the implosion.

This work supports a NIF experiment with the objective of investigating a foam ball target forming a shell. In the first stage of the experiment, a shock wave is launched that converges towards the center of the foam ball. For this proposed experiment, a laser pointing configuration was developed to address the fact that the beams of the NIF are not symmetrically arranged for direct drive and that 8 beams are needed to produce diagnostics for the experiment. This means that those beams cannot contribute to pulses driving the target. The angles of the beams were adjusted and tested through the 2D hydrodynamics simulation code SAGE to optimize the configuration for uniformity. To assess the uniformity of the implosion, the shock wave radius distribution was determined based on the laser energy distribution, allowing the uniformity of the shock wave velocity to be calculated. The new design gave a low nonuniformity value of 1.40%.

2. X-Ray Backlighting in the NIF Geometry

X-ray backlighting is a technique to produce radiographic images, especially of high-density phenomena.[6] These images allow scientists to see properties of the target during compression, and can help provide insight into how to improve the target's compression. As illustrated in Figure 3, this technique has some laser beams irradiating the backlighter, which emits x-ray photons. Other laser beams are irradiating the target for implosion. The x-rays from the backlighter pass through the target and some are blocked by the high density areas.[7] The x-rays must cross through the pinhole to the detector, because the surrounding substrate is made from a high Z material and is opaque to x-rays. An absorption image of the target's shape is created.

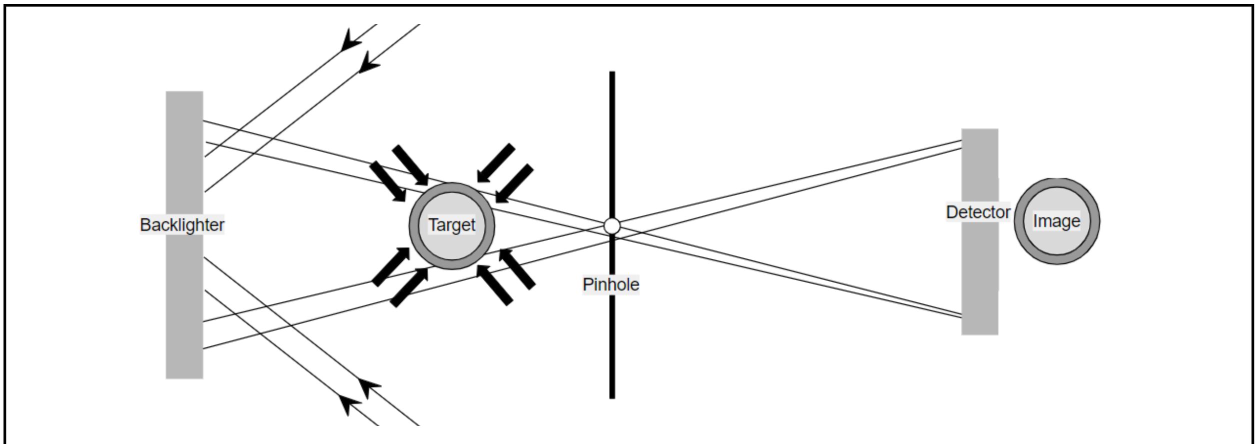

Figure 3: *Diagram of pinhole backlighting for a laser system.*

The NIF is structured with 48 quads and each quad contains 4 laser beams, summing to 192 beams overall. The structure of the NIF is shown in Figure 4 below, which is a two-dimensional projection of a spherical shell target with the laser beam configuration overlaid. The horizontal axis of Figure 2 is the vertical axis of Figure 4 since the hohlraum is oriented with its axis vertical on the NIF. In Figure 4, the beams are represented by green squares.The quads of the NIF are configured uniformly around the azimuth (φ) at angles of ϴ = 23.5°, 30.0°, 44.5°, and 50.0° from the poles, with corresponding angles in the lower hemisphere. All the quads around the target chamber at one angle are considered one ring, and there are 8 rings total. The rings are numbered 1–8 from top to bottom.

Although the NIF is primarily designed for indirect drive, a direct drive method would be used in this proposed experiment for a foam ball target. However, when the NIF is used for direct drive with all the beams hitting the target at normal incidence, the equator of the target is significantly underdriven in comparison to the poles.[8] This leads to the target being imploded into an ovoid shape as opposed to a uniform sphere. To counter this, polar direct drive was developed.[9] The beams are redirected towards the equator in order to drive the equator at the same rate as the poles. This method requires a different beam configuration on the NIF from typical direct drive. Figure 4 shows a configuration for polar direct drive on the NIF that was used for a previous backlighting experiment.[10]

In this NIF laser configuration, two quads which have eight beams total are used for backlighting. This means that these eight beams will not contribute to the target's implosion, and that the regions where the beams were aimed will have a lessened compression. This results in an implosion that is further away from the ideal uniformity. The currently used solution to this issue involves increasing the laser beam intensity for the 8 beams surrounding each backlighter quad by a factor of 50%. The aimpoint for each beam on the target is shown through a black dot. The black arrows show which beam is directed towards which aimpoint. The aimpoints of these 8 backlighting beams in each hemisphere are shifted to help compensate for the under-compressed regions.

Figure 4 shows contours of the center-of-mass radius of the imploded target after 6 ns. This is a representative time near the end of the laser pulse in the implosion experiment considered by Ref. 10, at which the center of mass radius was driven to 630 μm on average. The areas highlighted in red have a lower radius and have been compressed more while the areas highlighted in blue have a larger radius and have been compressed less. The root mean square (RMS) gives a value of the nonuniformity where the ideal would be 0%. This design has a 1.6% RMS for the center-of-mass radius, which is relatively low. The majority of the target is within 10 μm from the 630 μm mean, so the contour is $\frac{10}{630}$ or 1.6% from the mean. Over the whole sphere, the average deviation also ends up being 1.6%.

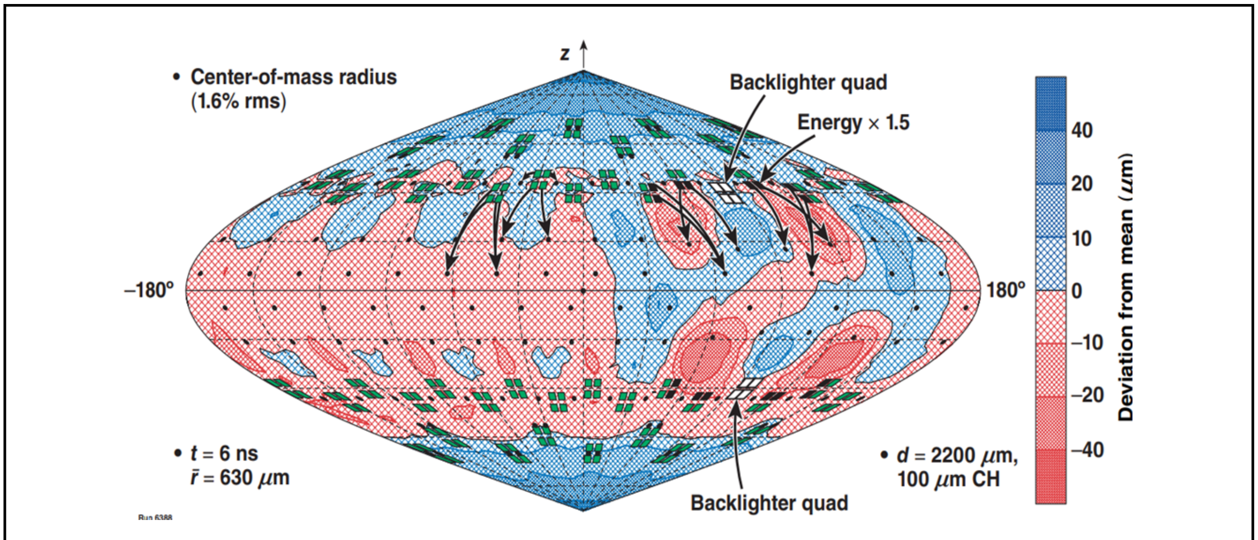

Figure 4: *Current NIF laser configuration with backlighters. The contours give deviations from the mean center of mass radius when the mean radius is 630 μm [From Ref. 10]*

However, there is a drawback to this current design. The energy of the 16 beams with increased intensity must stay below a certain limit to avoid the risk of laser system damage. As a result, the energy of the rest of the beams has to be lower than the limit by a factor of 1.5, leading to a lower overall energy compared to one without backlighting. In this work, a preferred laser configuration was developed with all the laser beams at the same intensity so this does not become an issue. To achieve this, simulations using different laser aimpoints were run and analyzed to identify a configuration that gives an optimally uniform result.

3. The Stages of a Foam Ball Implosion

For the proposed NIF experiment, a foam ball target would be used instead of the conventional target. The eventual goal is to use foam ball targets wetted with DT fuel. However, this proposed experiment is intended to first see how the concept of foam itself fares.[11] Liquid DT is absorbed into the foam, whereas conventional targets require forming a uniform solid layer of DT.[5] This also means that a shell in the foam ball must be formed after the start of laser irradiation, since it is not created in advance like conventional targets.

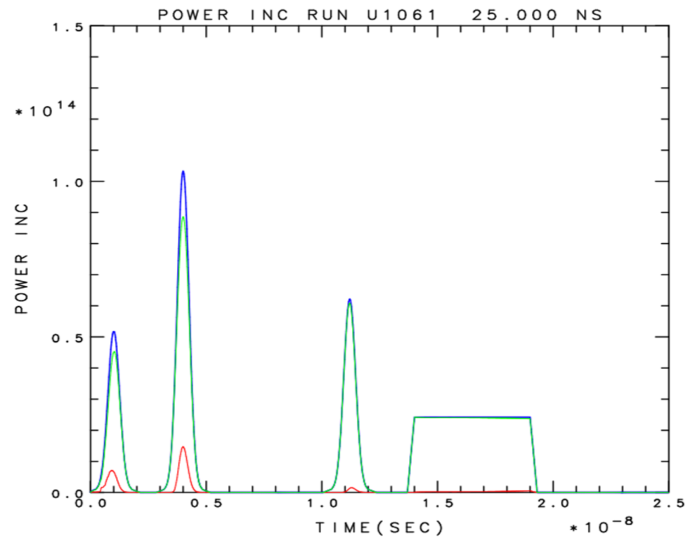

Figure 5: *Laser pulse design for proposed NIF experiment. Blue represents the amount of incident laser power; green represents the laser power absorbed by the target; red represents the laser power scattered.*

Figure 5 shows the power of the laser pulses in Watts on the y-axis with respect to time, throughout the 25 ns period. The short and intense laser pulses are known as pickets. In the figure, the blue line shows the amount of incident laser power. Of this power, most is absorbed by the target as shown by the green line and some is scattered as shown by the red line. In this experiment, only a small fraction of the laser energy is scattered and not absorbed by the target.

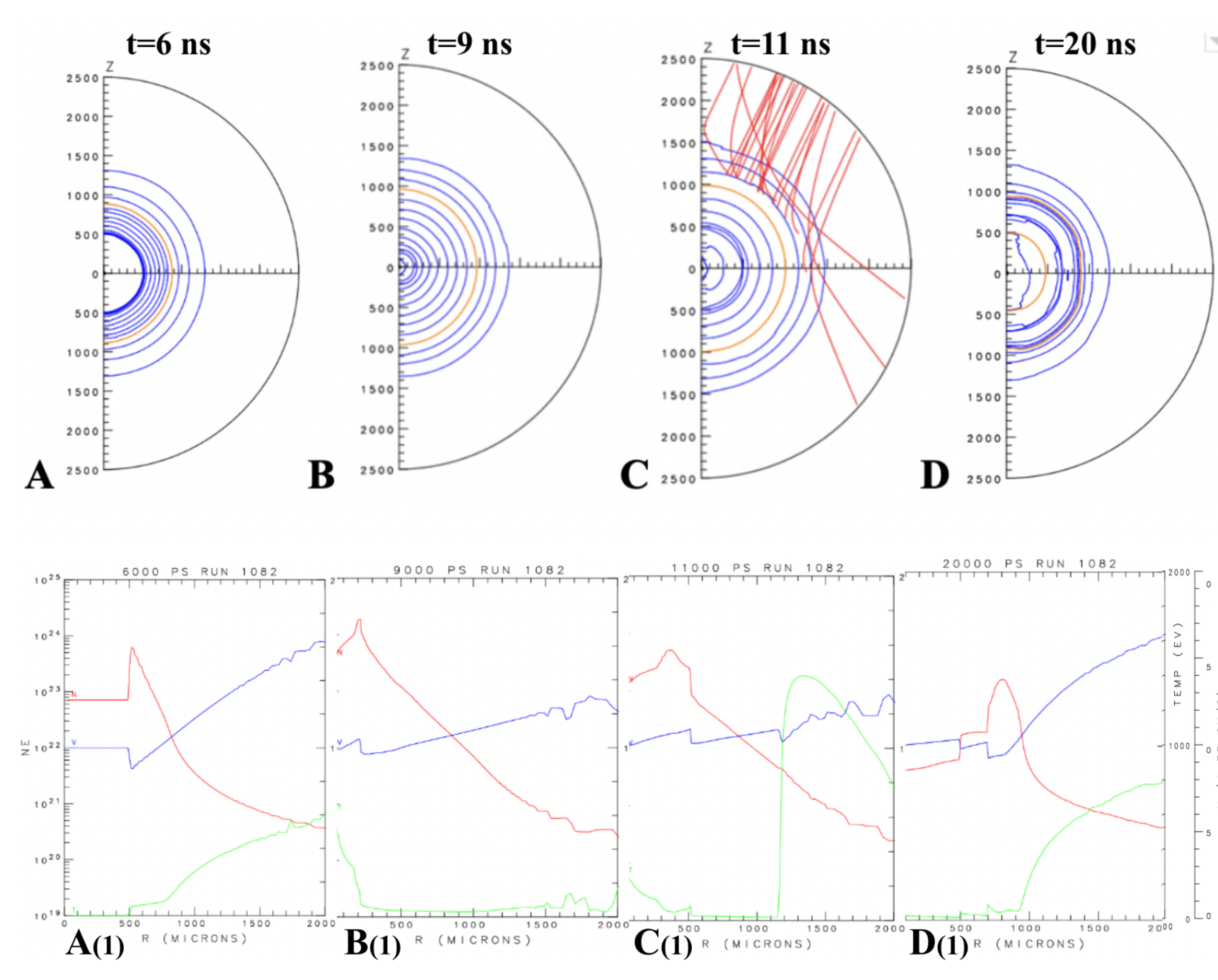

Figure 6: *A–D are density contours at selected times of the foam ball target during the proposed laser experiment; A(1)–D(1) are one-dimensional lineouts at 45° to the z-axis graphing the density in red, velocity in blue, and temperature in green throughout the depth of the foam ball target in μm at the same selected times. A: Initial compression; B: During expansion; C: Expansion stops; D: Final compression.*

The top row of Figure 6 shows density contours at different stages of the foam ball. The bottom row has lineouts of density (electrons/cc) in red, velocity (cm/s) in blue, and temperature (eV) in green. The target has a radius of 1100 μm to enable the pointing design of Ref. 10 to be used. (The pointing design depends on the target radius.) Stage A is at 6 ns, just after the first two pickets. The yellow contour line in Figure 6A–6D represents critical density, the greatest density that the laser rays can reach. Each contour line represents a factor of 2 in density. The foam deeper than the critical density line has an increased density, whereas the foam outside has a lower density. Figure 6A shows how the shock from the laser pulses reaches about 500 µm, which is also where the jump in temperature from 0 eV to around 50 eV and spike in density are. At this point around 500 µm, Figure 6A(1) shows that the velocity is negative compared to its starting value, signifying that the target is being compressed. Inside this shock front, the foam is undisturbed.

After stage A, there is a period where the picket pulses are paused. Stage B is at 9 ns, right before the third picket. The shock has converged at the center. The velocity is positive up to 200 µm as graphed in Figure 6B(1), showing that the shock has now bounced from the center outward. The plasma in the outer part of the target continues to expand. Stage C is at 11 ns at the peak of the third picket. The target has continued to expand but its expansion is stopped by this third picket. The laser rays illustrated in Figure 6C are from a beam incident at 23.5° from the top. Rays refract along curved paths and after losing energy to 1%, the rays are no longer plotted. This occurs at half the critical density. The target absorbs close to 100% of the rays that it is hit with, as shown by the green line in Figure 5.

Stage D is at 20 ns at the end of the pulses. The foam has been compressed again by the final laser pulse and a shell is identifiable at around 750 µm. The density in the region of the shell is higher according to Figure 6D(1). This is the point at which it is most useful to take a backlighting image to determine whether a shell was successfully formed.[11] The goal of the proposed NIF experiment is to confirm and image the formation of a shell in the target. In the future, it would take additional pulses to compress that shell or attempt reaching ignition.

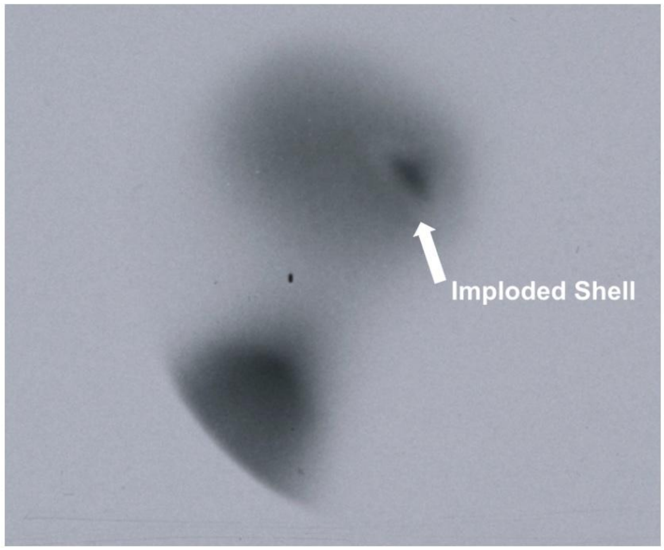

Figure 7: *Backlighting image of a foam ball implosion on OMEGA; Image credit to Dr. Christian Stoeckl and Dr. Igor Igumenshchev.*

Backlighting results for a foam ball implosion on a small scale were obtained on OMEGA in August 2022. In Figure 7, the imploded shell is visible as a slightly lighter ring around the darker part of the image. Obtaining similar results on a larger scale showing the formation of the shell is the goal of the proposed NIF experiment.

In the OMEGA experiment, the OMEGA EP laser was used as the backlighter. This meant that all the 60 beams from the OMEGA laser were able to be used for the implosion and the typical symmetrical configuration was used. However, the NIF does not have a separate laser that can be pointed to serve as a backlighter, and therefore two quads from the original NIF configuration have to be used as backlighters.

4. Beam pointing and focusing optimization

If no changes are made to the laser beam aimpoints of the NIF relative to the aimpoints with all quads present, there will be a significant decrease in laser energy deposited in the spots on the target that would have been irradiated by the backlighters. By adjusting the angular positions of the laser aim points in the φ direction, this issue was resolved. Logically, the beams closest to the backlighters would have to be shifted more than the beams further away in order to compensate successfully.[12]

Only the laser beams in rings 4 and 5 had backlighting beams. Therefore, those were the only rings with laser beam pointings adjusted. There was natural vertical and horizontal linear symmetry present in the NIF laser beam configuration that could be used to make the optimization process more efficient. A φ angle value was assigned to a specific laser beam aimpoint in ring 4 that would then be reflected for the correlated aimpoint on the opposite side. This concept for ring 4 is illustrated in Figure 8 and matches the ring 4 quads shown in Figure 4. For example, the symmetry about quad A', the backlighting quad, was used so that the same φ6 and φ7 are used for both D and D' with their directions reversed. The φ angle values from ring 4 were also used for ring 5, but reflected going from the upper to the lower hemisphere. To find the optimal design, there are 7 parameters (φ angles 1–7) that must be adjusted. Due to the vast number of possible combinations, a systematic approach was taken, starting with evenly spaced aimpoints. Each laser pointing configuration was run through the hydrodynamics code SAGE to calculate the RMS value for the uniformity.

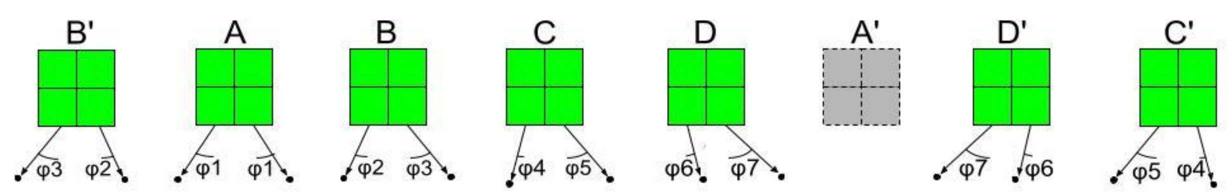

Figure 8: *Azimuthal pointing diagram of ring 4 quads, showing the symmetry of φ angles 1–7. Quad A' is used for backlighting.*

When all laser beams are in use, there are 32 beams in each of rings 4 and 5. In this design, only 28 beams from each ring are in use, and they are spread across the same 2π radians of the spherical target circumference. The new φ angles were first calculated so that each laser aimpoint in rings 4 and 5 was equally spaced out in the φ direction, as was proposed for an earlier experiment using backlighting in Ref. 13. This meant that the aimpoints had a π/7 radian spacing between them.

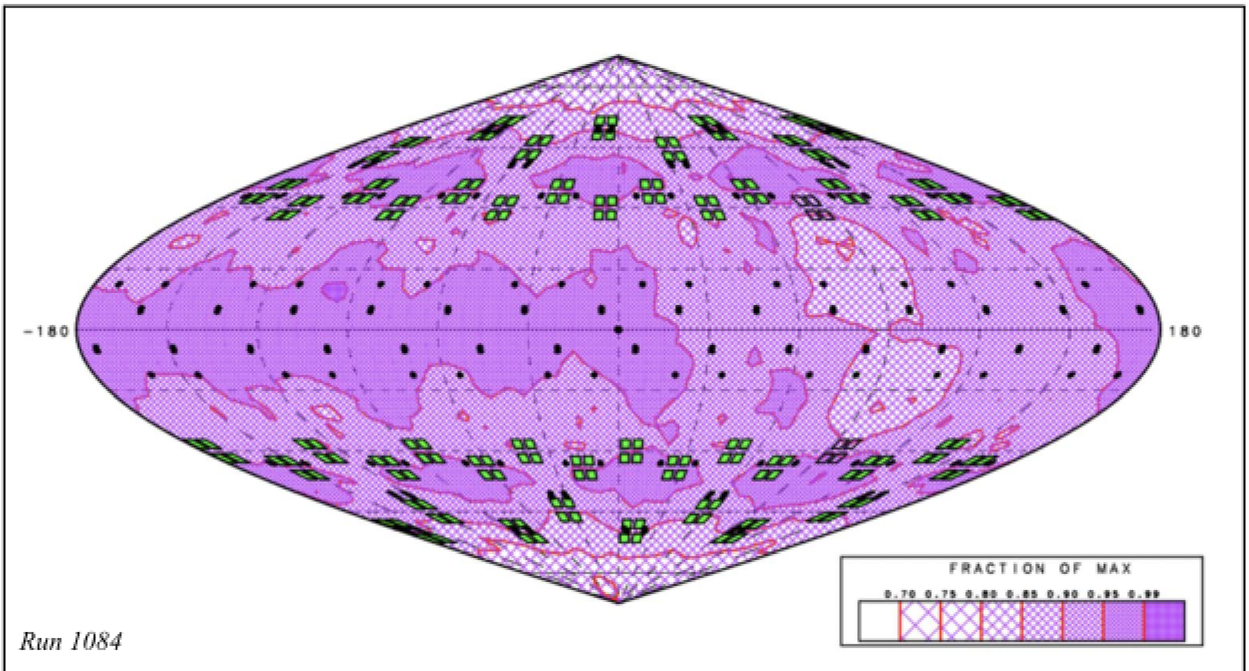

Figure 9: *Contours of deposited laser energy as a fraction of the maximum. The ring 4 aimpoints are uniform in φ with a π/7 radian spacing. The RMS is 3.93%.*

However, evenly spaced aimpoints in the φ direction did not cause an evenly distributed energy deposition in the φ direction. As shown in Figure 9, the beams that were aimed near the backlighters deposited approximately 85-90% of the energy the other beams in the same ring deposited elsewhere. The decrease in this region is because those laser beams had to shift further in the φ direction, which meant that the energy deposited from those beams was lower. These rays hit closer to the edges of the target rather than the center, leading to the target absorbing less energy. The RMS uniformity of the deposited energy for this simulation is 3.93%.

To produce a more uniform distribution of energy, combatting the weakened energy deposition in the backlighting region is necessary. Designs were investigated that had the aimpoints in that region closer together, by increasing the other aimpoints' spacing. A range of aimpoint spacings were simulated starting from the previously tested π/7 radians up to π/6.6 radians apart. This increase in spacing kept all the aimpoints of the quads the same distance apart except for quads D and D' whose aimpoints became increasingly closer together.

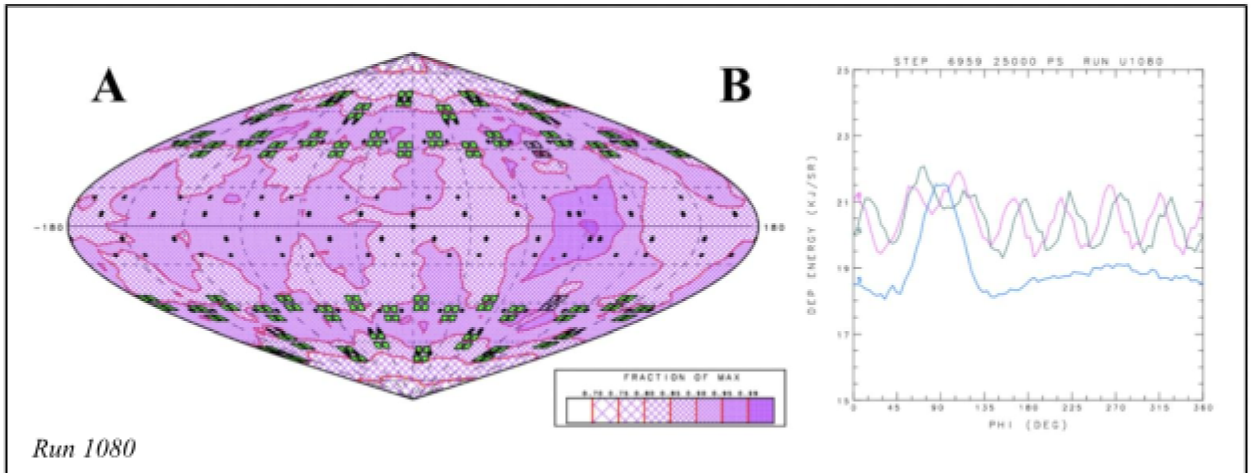

Figure 10: (A) *Target uniformity of deposited laser energy with a π/6.6 radian spacing. The horizontal dashed line above the equator is at 70° and the line below is at 110°.*
(B) *The energy deposition variance over the φ direction at specific θ angles. The green represents 110°, blue represents 90°, and pink represents 70°.*

Figure 10A shows that the backlighting region has been overcompensated at around φ = 90° in the π/6.6 radian spacing design. (In Figure 10A, φ = 0 occurs at the central meridian while in Figure 10B, φ = 0 is marked on the left side.) The two aimpoints close to the backlighting quad are close together as illustrated in Figure 10A. The uniformity variance for this pointing configuration is 3.53% RMS. Figure 10B shows the energy deposition variance for scans over φ at specific θ angles. The green represents 110°, blue represents 90°, and pink represents 70°. It is apparent that there is a spike in energy deposition around 90° in the φ direction, especially in the 90° θ lineout as shown highlighted in blue. This is approximately the location of the backlighting quads.

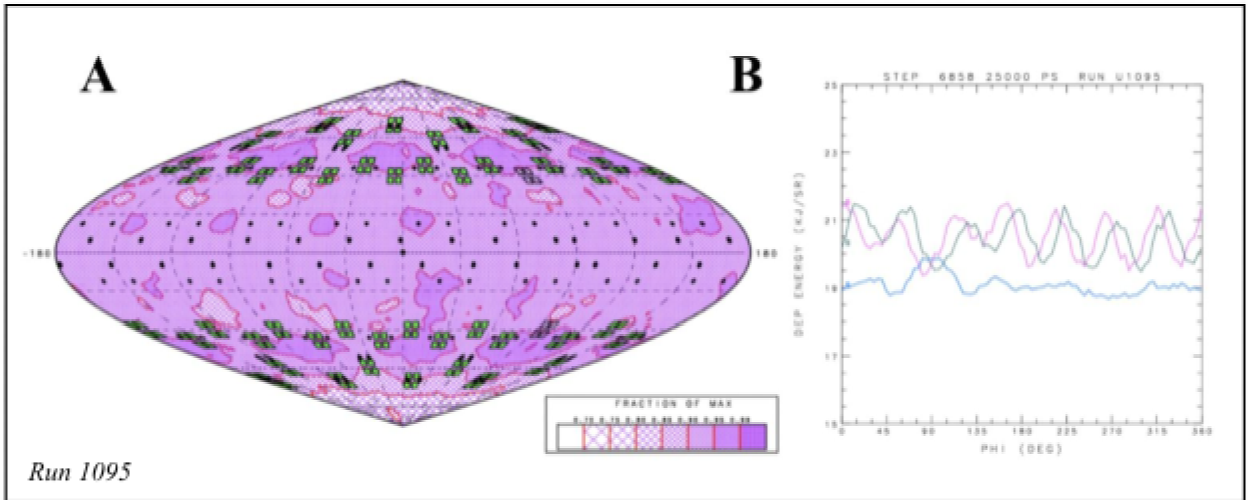

Figure 11: (A) *Target uniformity of deposited laser energy with a π/6.8 radian spacing* (B) *The energy deposition variance over the φ direction at specific θ angles. The green represents 110°, blue represents 90°, and pink represents 70°.*

Figure 11A shows a simulation run with a π/6.8 radian spacing. The energy deposition is slightly more uniform, with an RMS of 3.38%. Figure 11B shows that each θ lineout vs φ is more uniform compared to the other simulations, because there are no major dips or spikes. However, the azimuthal angle adjustments only made a small difference to improving the RMS, because the nonuniformity in the θ direction is also a contributor. As in Figure 10B, the lineout at θ = 90° has a lower average energy deposition than the lineouts at the other values of θ. This is expected as ring 4 is aimed towards the equator and there are 7 quads available rather than the 8 assumed by the previous pointing design.

Additionally, minor adjustments in the φ direction on top of the π/6.8 radian spacing were experimented with to increase the optimization. The values of φ1 – φ7 used are shown in Table 1. This adjustment produced the optimized design.

Table 1: *Aimpoint φ angles for beams in rings 4 and 5, including minor adjustments*

φ1	φ2	φ3	φ4	φ5	φ6	φ7
14.74°	3.79°	22.68°	4.35°	31.12°	8.59°	40.06°

5. Assessment of Overall Uniformity

Figure 4 used the center of mass radius to assess the overall uniformity of an imploding shell of a conventional target. However, this same concept cannot be applied to a solid such as the foam ball target. Foam ball targets do not have a clear change in density to identify the center of mass radius. Instead, the shock radius is used, as shown in Figure 6A. Identifying the shock radius can be done by finding the radius at which the temperature increases to 10 eV. This can also provide a more accurate representation of the uniformity of the target as time passes.

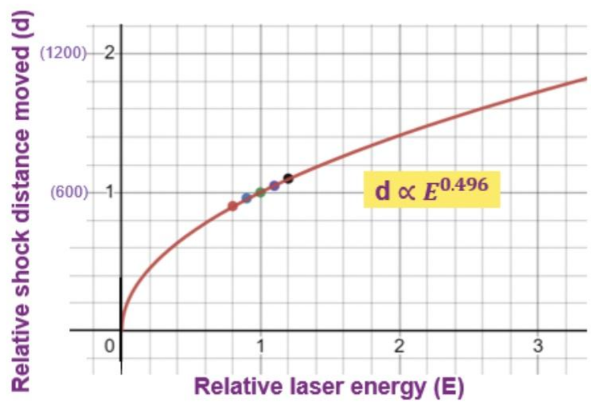

Figure 13: *The proportional relationship between shock distance moved and laser energy is graphed*

SAGE is a two-dimensional hydrodynamic code that calculates the radius and θ dependence of the implosion. However, it needs to be able to relate the deposited energy to the shock wave distance moved in order to calculate the φ dependence of the implosion. Thus, the relationship between laser energy and shock distance moved was investigated. To estimate this relationship, multiple simulations were run from 80% to 120% of the original total laser energy, with a 10% incrementation each run. It was found that there was a scale factor of 0.496 connecting the two proportionally as shown in Figure 13. Previous work used a similar method to relate the distance moved by the imploding shell to the amount of laser energy.[14] The two were determined proportional by a scale factor of 0.72. This factor for the distance moved by the imploding shell is greater than the factor for the distance moved by the shock.

The scale factor of 0.496 was then used to create a shock wave radius plot (Figure 14) from the energy deposition distribution plot. The shock wave radius deviated 8.4 μm on average from the average 600 μm distance moved. The RMS velocity nonuniformity, the mean difference from the average velocity across the shockwave, for this plot is therefore 1.40%.

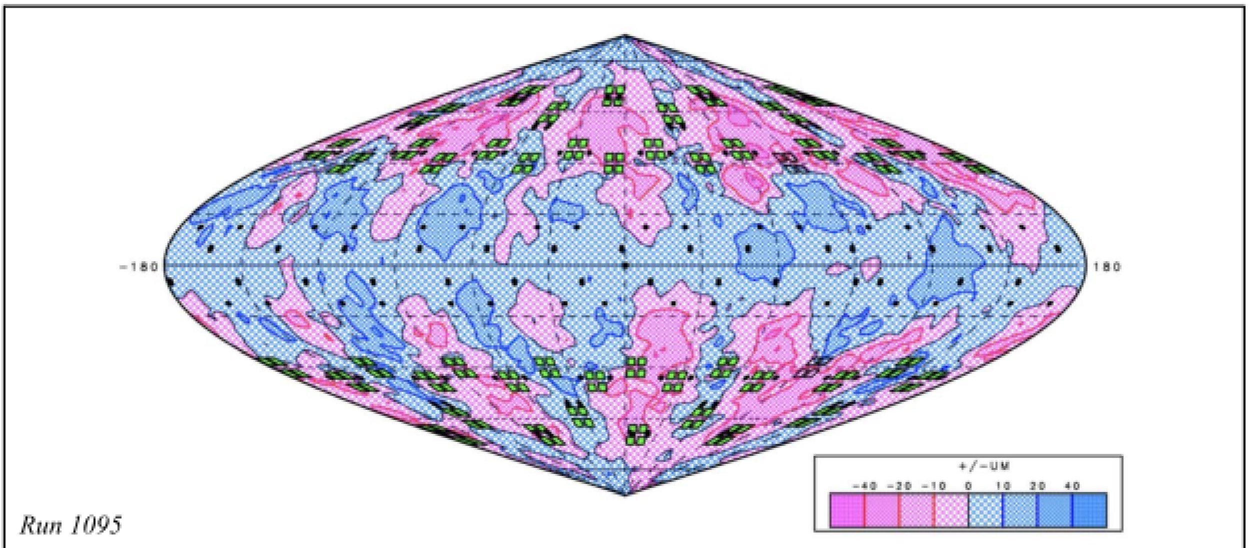

Figure 14: *Contours of deviation from the average of the shock wave radius of the optimized design at 6 ns, when the shock has moved 600 μm to an average radius of 500.5 μm. The RMS is 1.40%.*

Conclusion

This work developed an improved configuration for a proposed experiment on the NIF to irradiate a foam ball target and produce a highly uniform implosion while using two quads for backlighting. Foam ball targets have potential applications in future fusion energy plants. They are desirable when a mass supply of targets is necessary, because the formation of the shell can occur right before implosion, rather than during the preparation of the target. Backlighting is necessary to determine the success of the shell formation during the proposed experiment on the NIF. This will allow the practicality of foam ball targets to be assessed for future experiments.

The current design for backlighting on the NIF increases the intensity and shifts the beams surrounding the backlighting quads in order to compensate. The rest of the beams are not adjusted. In the improved design developed here, all the beams are at the same intensity and the entirety of beams in rings 4 and 5 are shifted around the azimuth. The improved design has the advantage that the target can be irradiated with a 50% higher energy. Beyond foam ball target experiments, other experiments that use the current pointing design to produce backlighting images on the NIF can benefit from using this new design.

Acknowledgments

I would like to give my appreciation to my advisor and the program director, Dr. R. Stephen Craxton for helping me immensely throughout my project. I would also like to thank Dr. Igor Igumenshchev for showing me his simulations of foam ball targets. I appreciate Ms. Kim Truebger for helping the program run smoothly. Lastly, I would like to acknowledge my parents for their support.

References

1. I. Hoffman. “Review of Accelerator Driven Heavy Ion Nuclear Fusion.” Matter and Radiation at Extremes. *3*, 1 (2018).
2. J. Nuckolls, L. Wood, A. Thiessen, and G. Zimmerman. “Laser Compression of Matter to Super-High Densities: Thermonuclear (CTR) Applications.” Nature, *239,* 139 (1972).
3. J. D. Lindl. “Development of the Indirect-Drive Approach to Inertial Confinement Fusion and the Target Physics Basis for Ignition and Gain.” Phys. Plasmas, *2,* 3933 (1995).
4. *International School of Quantum Electronics 54th Course: “Atoms and Plasmas in Super-Intense Laser Fields”* http://www.emfcsc.infn.it/ef/emfcsc2013/posters2013.html (2013).
5. V.N. Goncharov, I. V. Igumenshchev, D. R. Harding, S. F. B. Morse, S. X. Hu, P. B. Radha, D. H. Froula, S. P Regan, T. C. Sangster, and E. M. Campbell. “Novel Hot-Spot Ignition Designs for Inertial Confinement Fusion with Liquid-Deuterium-Tritium Spheres.” Physical Review Letters, *125*, 065001 (2020).
6. O. L. Landen, D. R. Fraley, S. G. Glendinning, L. M. Logory, P. M. Bell, J. A. Koch, F. D. Lee, D. K. Bradley, D. H. Kalantar, C. A. Back, R. E. Turner. “X-Ray Backlighting for the National Ignition Facility.” Review of Scientific Instruments. *72,* 627 (2001).
7. R. VanDervort, M. Trantham, S. Klein, C. Sorce, P. Keiter, and R. Drake. “Development of a Backlit-Multi-Pinhole Radiography Source.” Review of Scientific Instruments. *89,* 10G110 (2018).
8. A.M Cok, R. S. Craxton, and P. W. McKenty. “Polar-drive designs for optimizing neutron yields on the NIF.” Phys. Plasmas. *15*, 083705 (2008).
9. S. Skupsky, J. A. Marozas, R. S. Craxton, R. Betti, T. J. B. Collins, J. A. Delettrez, V. N. Goncharov, P. W. McKenty, P. B. Radha, T. R. Boehly, J. P. Knauer, F. J. Marshall, D. R. Harding, J. D. Kilkenny, D. D. Meyerhofer, T. C. Sangster, and R. L. McCrory. “Polar Direct Drive on the National Ignition Facility.” Phys. Plasmas. *11,* 2763 (2004).

10. R. S. Craxton, M. Hohenberger, W. E. Kehoe, F. J. Marshall, D. T. Michel, P. B. Radha, M. J. Rosenberg. “Design of Platforms for Backlighting Spherical Implosions on OMEGA and the NIF.” 58th Annual Meeting of the American Physical Society (2016).
11. V. Goncharov, L. Ceurvorst, S. Craxton, I. V. Igumenshchev, M. Rosenberg, W. Theobald, W. Trickey. “Demonstration of High-Density Shell Formation Dynamically Starting from a Homogenous Density Ball in Support of the Dynamic Shell Ignition Concept.” Unpublished proposal (2022).
12. W. Kehoe. “Beam Pointing Optimizations for Omega Implosions.” Laboratory of Laser Energetics High School Program (2016).
13. N. S. Krasheninnikova, S. M. Finnegan, and M. J. Schmitt. “An Initial Assessment for Three-Dimensional Polar Direct Drive Capsule Asymmetries for Implosions at the National Ignition Facility.” Phys. Plasmas. *19,* 012702 (2012).
14. L. Tucker. “A Design for a Shock Ignition Experiment on the NIF Including 3-D Effects.” Laboratory of Laser Energetics High School Program (2011).